Engineering Science and Technology, an International Journal 34 (2022) 101090

HOSTED BY

Contents lists available at ScienceDirect

Engineering Science and Technology, an International Journal

journal homepage: www.elsevier.com/locate/jestch

Biotribology of synovial cartilage: Role of albumin in adsorbed film formation

Pavel Čípek *, Martin Vrbka, David Rebenda, David Nečas, Ivan Křupka

Department of Tribology, Faculty of Mechanical Engineering, Brno University of Technology, Technická 2896/2, Brno 616 69, Czech Republic

ARTICLE INFO

Article history:
Received 9 June 2021
Revised 30 November 2021
Accepted 23 December 2021

Keywords:
Biotribology
Cartilage
Reciprocating tribometer
Friction
Lubrication
Fluorescence microscopy

ABSTRACT

A properly lubricated natural synovial joint is the basis of the proper function of the natural musculoskeletal system to lead an active and painless life. A properly lubricated natural synovial joint is the basis of the proper function of the natural movement system to lead an active and painless life. Well lubricated synovial joints are expressed, in particular, by an extremely low coefficient of friction and wear between cartilage surfaces. The presented manuscript is focused on the impact of albumin protein on the formation of adsorbed boundary layer in the contact of cartilage – a simplified model of synovial joint. This can contribute to better understanding of the lubrication in synovial joints. All presented experimental tasks were performed using a reciprocating tribometer along with fluorescence microscopy – friction forces were measured simultaneously with fluorescence records of contact. This unique experimental approach used a newly designed evaluating procedure based on image processing. The experimental results show a great impact of hyaluronic acid; adding of hyaluronic acid leads to a reduction in friction and a larger area of albumin adsorbed boundary layer; however, the phospholipids show the opposite effect. A combination of the individual protein solutions, albumin and γ-globulin, has no significant effect on the particles count of albumin clusters adsorbed in the contact; however, the area of albumin adsorbed boundary layer with simple albumin solution was much larger than the solution combining both proteins. The conclusions and discussion of this study describe the role of albumin protein in the lubricating process prevailing in a simplified model of synovial joint under conditions corresponding to slow human gait.

1. Introduction

The comfortable and active human life needs a proper functioning of the musculoskeletal system; however, despite a high level of current state of healthcare, we suffer from a number of joint diseases [1]. The progression of joint diseases may vary depending on many factors and can reach the state when the joint is incurable. So far, the most common solution for the incurable natural joint is its removal and replacement by an artificial one [2]. Although the advanced joint prosthesis has a long lifetime, sometimes it has to be replaced repeatedly. A reoperation of the prosthesis is a considerable burden for the human body. It has the impact on bone degradation, mental health of patients, etc. [3–5]. This is enormously stressful for people who prefer an active life but are afraid of reoperation; therefore, the general effort is to postpone the necessity of operation of prosthetics as long as possible.

One of more contemporary ways of how to treat or, at least, delay or stabilize the disease of the natural joints which are not completely destroyed, is a non-invasive treatment (the intervention does not require surgery) using viscosuplementation (supplement – a gel-like fluid consisting mostly of hyaluronic acid (HA) is injected into the joint gap) [6]. Due to the limited lifetime of the prosthesis, the common endeavor of viscosuplementation is to defer the urgency of operation of prosthetics as long as possible. The supplements should restart the lubrication processes in degraded natural joints, which ideally stops future damaging of joints or, at least, slows down the process of degradation of natural joints (natural cartilage) [6,7]. The supplement therapy is usually effective, but the same therapeutic effect is not guaranteed for all patients, and how exactly the supplement works has not yet been proven [8–10]. To better understand this issue, the full principle of lubrication in natural synovial joints needs to be described, i.e., it is necessary to describe the adsorbed boundary layer formation in

* Corresponding author.
E-mail address: Pavel.Cipek@vut.cz (P. Čípek).
Peer review under responsibility of Karabuk University.

https://doi.org/10.1016/j.jestch.2021.101090

the contact realized by the articular cartilage and lubricated by synovial fluid (SF) [11].

The basis of the unique tribological and mechanical properties of natural synovial joints is the contact of two bones, whose surfaces are covered by the articular cartilage, and the lubrication is realized by SF [12]. Due to the specific mechanical and tribological properties of cartilage, the contact pressure is dispersed over a large area on the surface of cartilage where the SF ensures a very low friction coefficient (CoF) [13]. An alternative to a natural cartilage is a hydrogel, which represents an artificial model of cartilage with similar tribological properties [14]. Most of natural cartilage tissue consists of water and of type II collagen fibres as a matrix, HA, and lubricin [12,15]. The tissue of a fabric structure is filled with water and its thickness is divided into three zones, varying especially in orientation, shape, and amount of collagen fibres [12,16]. The cartilage tissue is characterized by low cell density; therefore, the tissue of cartilage is nourished through the SF [17]. The SF is mainly formed by proteins, HA, phospholipids and proteoglycans [18–20]. Based on the study [20], the albumin protein is the most abundant in the SF. The porous cartilage structure contains negatively charged components which provide the attraction and detention of water (SF) to the pores [21]. The lubrication system in natural synovial joints works on the principle of porous structure and absorption of water, on which is based the synovial joints lubrication system. There are many theories which seek to explain this principle, but so far there is no work that would give a comprehensive overview of the lubrication function in the synovial joint.

The research focused on tribology of cartilage can be divided into two main groups. The first one is focused on cartilage lubrication and the other one describes the friction performance of cartilage. The main discussed topic in the lubrication studies is the lubrication regime, where there are several theories attempting to explain the lubrication mechanism including hydrodynamic lubrication [22], boundary lubrication [23,24], weeping lubrication [25,24], and boosted lubrication [26]. Some studies published in later years show more advanced lubrication theories or present new theories of lubrication mechanisms – hydration lubrication [27], and adaptive multimode [28,29]. Although the studies on visualization are less common, the published ones mostly describe the use of hydrogel instead of cartilage. These studies seek to support and verify the mentioned theories, and the authors try to classify the influence of individual components of SF. The γ-globulin protein was shown as a significant component in the lubrication process of hydrogel; nevertheless, a degree of influence depends on the γ-globulin protein concentration and the concentrations of remaining components of the lubricant [30]. The gel–like layer on the surface of cartilage is also essential for lubrication processes, because it can protect the surface from wear. HA is the main component of gel-like layer. This layer is formed on the cartilage surface due to bonding of HA with chondrocytes contained in the structure of cartilage [31]. The thickness and composition of gel-like layers depend on the size of individual molecules and the pore sizes. Large molecules cling to the surface of cartilage and the cartilage structure is penetrated only by smaller particles. [32]. All presented studies reflect the fluid leakage from the cartilage structure, which is the basis of all theories.

Another topic discussed by the researchers is focused on the friction properties of cartilage. The "friction" issues of cartilage are better understood due to a simpler but more developed methodology related to the experiments and evaluation of data. These "friction" studies indicate the understanding of cartilage behaviour due to friction. They deal with the behaviour of cartilage contact lubricated by SF and indicate very good friction properties [33,34,35], which is expressed by very low CoF. The positive impact of friction (lower CoF) may be expressed by a larger volume of HA in SF [34], rehydration [36], higher load [33,37,36]. There is the dependence between the level of CoF and the type of movement [37]. The change of the sampling point on the cartilage surface has a significant impact on CoF; this depends on the mechanical properties of cartilage samples [38]. The general CoF trend has a growing character [33,34,37].

As is obvious, many studies are focused only on friction of cartilage contacts while the studies dealing with visualization are less common. Moreover, there are no studies connecting these two issues into one experimental task; i.e., the experimental device and methodology, which allow for simultaneous measurement of friction forces and visualization of cartilage contact (a simplified model of synovial joint). Some authors used a fluorescence microscopy for visualization of cartilage or hydrogel contacts, from which it follows that this method is the most appropriate for the visualization of compliant (cartilage) contacts on non-reflective surfaces. Studies dealing with visualization of cartilage contact are not frequent and the link with measurement of frictional forces is missing. The present study supplements the relationship between the cartilage visualization and friction measurement in the simplified model of synovial joint; therefore, a better description of cartilage lubrication processes will be replenishing, which can help to better understand the cartilage lubricating processes. The previous study [39] presents the methodology for the evaluation of simultaneous visualization of cartilage contact together with friction measurement. This study is a follow-up one and extends the research dealing with the experimental task focused on the behaviour of albumin protein in the formation of adsorbed boundary layer in the cartilage contact and the methodology presented in [39] is used. This study aims to clarify the link between the influence of albumin protein (as the protein with the highest concentration in SF [20]) in the formation of adsorbed boundary layer and the change of CoF trends. An explanation of the lubricating processes and the adsorbed boundary layer formation in the synovial joint contact can contribute to understanding of viscosupplements function and ensuring the right effect on all patients.

2. Materials and methods

2.1. Experimental device

A pin-on-plate tribometer of a unique own design was used as described in detail in [39–41]. The basis of the experimental device (schema is shown in Fig. 1A) is a cartilage sample in contact with a reciprocating glass plate (material B270). The contact is loaded using a lever through the cartilage sample and this is placed under the glass plate. The optical system is located above the contact and the observation record is obtained by camera. The contact is flooded with lubricant – in this case, the SF model. The lubricating bath is heated to the human body temperature (37C) by temperature controller Hotset C448 together with heating cartridges. These are placed under the bath and the temperature sensor is placed as close to the lubricant as possible. This arrangement prevents the lubricant from overheating (overheating of lubricant would cause rapid degradation of used components). A rigid frame of tribometer is the basis of the whole device and, together with the ball screw, allows for the reciprocating motion without clearance. The loading mechanism is based on the principle of a lever mounted on two preloaded bearings. The loading lever is equipped with a deformation member allowing for a minimum deformation in the loading direction and a high deformation in the friction direction, which permits the measurement of very low friction forces. Both forces (normal and friction) are measured by tensometric sensors. The reciprocating motion and loading are ensured by the stepper motors - rotational in the reciprocation case, and linear in the other

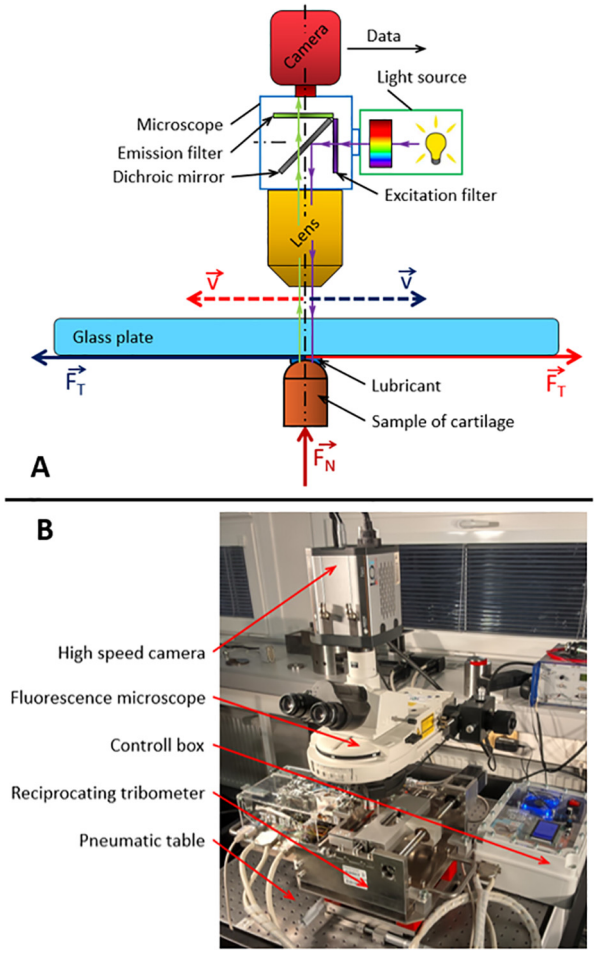

Fig. 1. Experimental apparatus. (A) schema of experimental apparatus, (B) experimental apparatus in laboratory.

case. The reciprocating tribometer is placed on the pneumatically balanced table, where the fluorescence microscope is also anchored. The entire experimental device is shown in Fig. 1B. The outputs of each experiment are the record of contact area and the friction and load forces trends.

2.2. Fluorescence microscopy

The fluorescence microscopy was used as an optical (observation) method for the experiments presented in this study. The basis of this method is a light emission of a substance excited by radiation. The fluorescence principle can be divided into three steps. First, it is excitation, when the excitation photon is absorbed by the fluorophore contained in the fluorescent dye. It is followed by the excitation state period; the absorbed energy is dissipated to ensure the emission of fluorescence. The last step is emission – the dye emits radiation; however, the level of energy is lower due to dissipation of energy in the excitation state period, which is the reason why the emitted radiation has a longer wavelength. A detailed description of fluorescence principle is shown in [42]. The mercury lamp allowing for the emission of a white light was used as a light source. The FITC and TRITC filters placed behind the mercury lamp were used to achieve the required wavelength of emitted and excited light for the dyes. The FITC filter has an excitation wavelength of 490 nm and the emission wavelength of 525 nm, the TRITC filter has an excitation wavelength of 557 nm and the emission wavelength of 576 nm. The optical method and the fluorescence microscope were described in detail in previous studies, where the methodology of visualization of joint replacement for different material combinations was published [43,42]. The visualization (recording of the contact area) is performed through the glass plate, the material of which ensures that the excitation and emission of the contact are not affected. The schema of the optical system is shown in Fig. 1A.

2.3. Specimens and lubricants

The femoral hip heads of mature pigs were utilized for samples removal. The area with the highest contact pressure on the surface of femoral head of hip joint was defined as a sampling area; this definition provides the most mechanical properties of cartilage sample. Due to a compliance of the same placement of removed samples (for all removed bones), the deviation between all samples was minimized, and the mechanical properties were comparable. The samples were removed by the ejector with internal diameter of 9.7 mm. The sampling was performed without delay after the slaughter of the animal. The samples were inspected after sampling with a focus on the preservation of the cartilage surface and on the cartilage edges damage (not to be frayed) to avoid influencing the experiments. The samples were deep frozen (−20 ℃) in phosphate buffered saline (PBS) immediately after sampling. Samples were defrosted immediately before the experiments to avoid degradation. Defrosting of cartilage samples was performed without heating at laboratory temperature, after that the sample is removed from the test tube and placed to the tribometer and flooded by lubricant. The same sampling process was verified in [44]. The sampling process used in this study is shown in Fig. 2. Due to the variability of cartilage samples, the samples were preselected before the experiments. The used cartilage sample was selected using a strict laboratory protocol. The second sample from the contact pair was the glass plate, which fulfils the important premise of transparency in order to observe the contact. The glass plate is 154 mm long, 43 mm wide, and 4 mm thick.

The model of physiological SF and its partial solutions were used as an experimental lubricant. The composition of synovial fluid was inspired by the native synovial fluid. The analysis of native synovial fluid was performed in [20] and the used composition of lubricants was inspired by this article. The variation and composition of all experimental lubricants are shown in Table 1. As is obvious from Table 1, the most represented component of synovial fluid is the albumin protein. Due to this fact, the albumin protein was defined as one of the most important components of synovial fluid; therefore, this article is focused on visualization and behaviour of albumin protein - the albumin protein was examined across all experiments. A bovine serum (BS) albumin (Sigma-Aldrich, A7030) was labelled by Rhodamine B isothiocyanate (283924, Sigma-Aldrich) in this case. The magnetic stirrer was used to stir the other components without dye with the labelled component. The other component of the experimental solutions was γ-globulin from bovine blood (Sigma-Aldrich, G5009), HA = Sodium Hyaluronate HySilk (powder, quality class-cosmetic; molecular weight = 820–1020 kDa, Contipro, Dolní Dobrouč, Czech Republic) and phospholipids = L - α - Phosphatidylcholine (powder, Type XVI-E, lyophilized powder; ≥ 99%; vesicles form; P3556, Sigma-Aldrich, St. Louis, MO, USA). The final solution was prepared by mixing all components with PBS solution. Solutions were mixed using a magnetic stirrer at a maintained laboratory temperature – without heating. The mixing process performs without air access (to avoid degradation) – the laboratory vessel is covered with a nontoxic parafilm foil. The process takes approximately 2 h, until all lubricant components are complete dispersion. The prepared protein solutions were kept in a deep-frozen state (−20 ℃) in opaque and darkened test tubes to prevent degradation and ordination

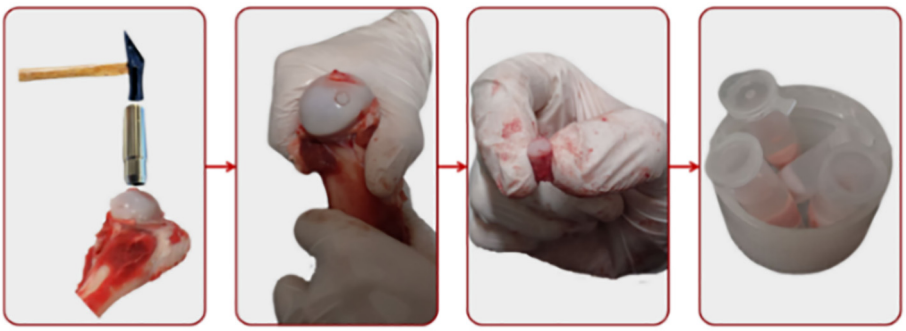

Fig. 2. Sampling process.

Table 1
Lubricants composition, labelled component - albumin.

Lubricant label	Albumin (mg/ml)	γ-globulin (mg/ml)	HA (mg/ml)	Phospholipids (mg/ml)
Lubricant 1	20	–	–	–
Lubricant 2	20	3.6	–	–
Lubricant 3	20	3.6	2.5	–
Lubricant 4	20	3.6	2.5	0.15

of lubricants. Defrosting was performed immediately before the experiments.

2.4. Methodology and conditions

The performed experiments followed a strictly defined procedure for preventing the undesired errors in the results and to help a sufficient repeatability of results. The established procedure of each experiment was described in detail in previous works [41,39]. The same experimental conditions were used for all performed experiments to make the results comparable, see Table 2. The conditions laid down are based on the presented studies in this field regarding the prevailing conditions in the natural synovial joint [45,46]. The load was set at 10 N, which corresponds approximately to 0.8 MPa of contact pressure and 10 mm/s of sliding speed. These conditions correspond to a very slow human gait and average joint pressure [45,46], which is a joint regime corresponding to a large part of human joint life. The experimental temperature was maintained at 37C. A similar condition was used for experiments in previously published studies; it allows to compare the results between this study and the studies that have already been published [34, [36]. Each experiment, i.e., the experiment with one type of lubricant, was carried out 9 times (3 experiments, where one experiment counts 3 repetitive experiments with an in - between hydration cycle, together with 9 individual experiments). The schema of one set of experiments is shown in Fig. 3. The selected count of experimental tasks allows to determine the repeatability of the experiments and the impact of rehydration. All experiments were performed on one sample so that the results of the individual experimental sections can be compared; especially, the recordings of the contact area. To ensure the same state of the cartilage sample before each experimental set, the run – in a cycle was carried out before each set of experiments, which helps to bring the cartilage structure and surface to the same state before each experimental section.

Output procedures are described in detail in the previous work [39]. The process to evaluate the results is shown in Fig. 4. As is obvious, the evaluation process is divided into two parts – CoF processing (Fig. 4A – C) and processing of the record of contact area snaps (Fig. 4D – G), which finally shows the dependency between friction and lubrication. The raw main data output from each experiment are friction forces measured in the contact and the record of the contact area through the fluorescence microscope. This data was further processed. The friction trend is transformed to CoF and is fitted by the straight line. The tangent slope is determined for each CoF trend and it is the evaluation value for the connection with lubrication.

The record of the contact area from each experiment whose output are the snaps, is an input for the processing by the specially designed software described in detail in [39]. This software is based on the principle of image segmentation, allowing for the removal of the background and highlighting particles that have an order of magnitude higher intensity. This processing ensures that only the marked particles to be monitored are left in the snap. The software calculates the particle count and the average size of particles in each snap. These values are determined for all snaps; therefore, the particle count trend was defined for each experiment. This trend is fitted by a straight line and the tangent slope was determined, whereby it is expressed as the relative difference of particle count and it is the output evaluation value from visualization, the second evaluation parameter.

The culmination of the evaluation process is the linking of both relative differences which form the final output from each experiment – dependency between the particle count and CoF. Both differences are relative to allow for a comparison between both output parameters and also between all performed experiments. The final CoF and the particle count dependency allows to determine the impact of the individual compositions of the lubricant on the lubrication process.

Table 2
Experimental conditions.

Load	Velocity	Stroke	Number of cycles	Duration	T
10 N	10 mm/s	20 mm	25	2 min	37 C

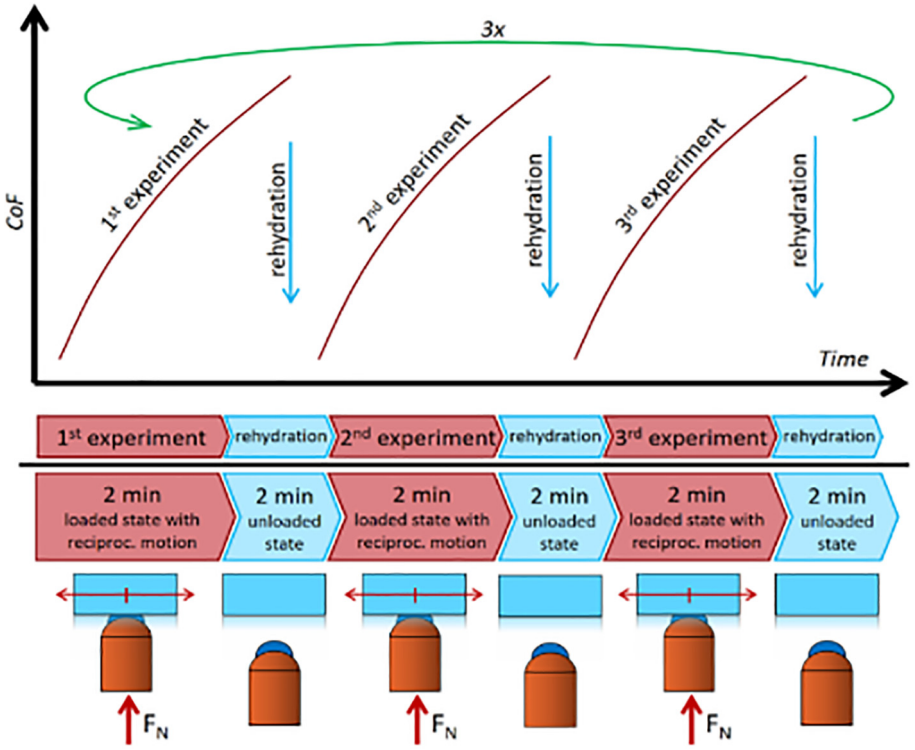

Fig. 3. Schema of each experimental set.

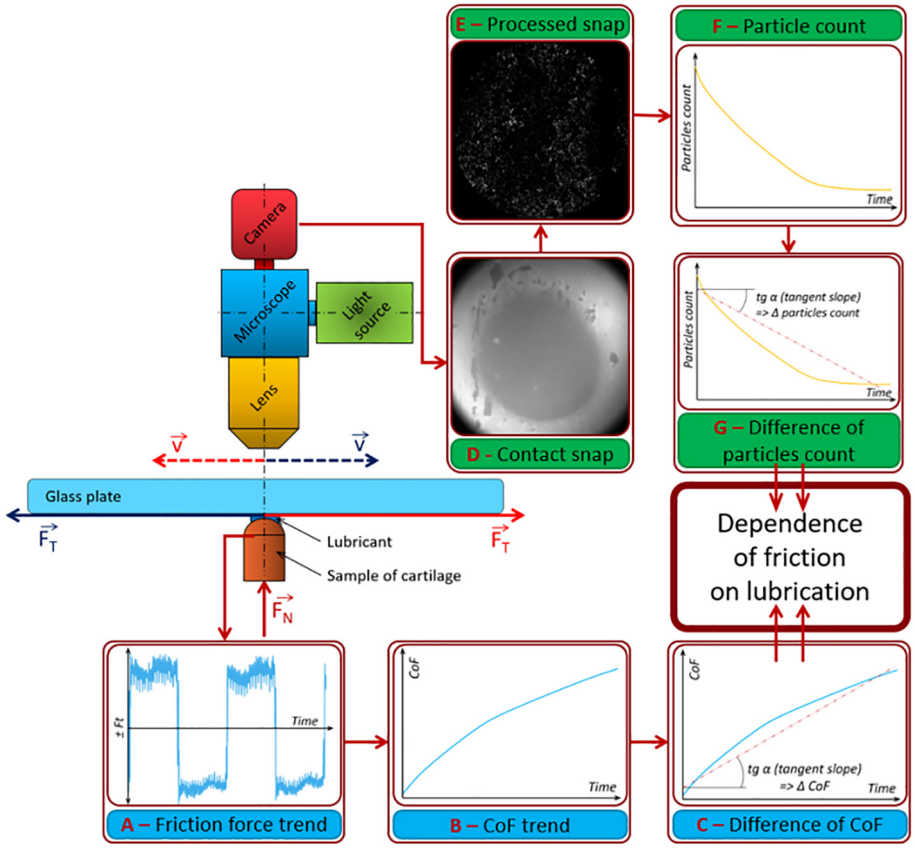

Fig. 4. Evaluation schema.

3. Results

3.1. The toolbar and its menus

Four sets of experimental tasks were carried out and each set was performed with one modification of lubricant (lubricant 1 – 4, see Table 1). Each lubricant was used for 3 replicate measurements consisting of 3 consecutive measurements with rehydration between each experiment, 9 individual experimental tasks in total (see Fig. 3). The friction trends for all modifications of lubricant are shown in Fig. 5. One curve in this graph represents 3 averaged measurements, and each type of curves represents one set of experiment (1,2,3) with in–between rehydration (see Fig. 3). The lowest fiction is reported by lubricant 3, although it is not the complex SF. However, the lubricant 4 (complex SF model - adding of phospholipids to the lubricant unlike a lubricant 3) causes deterioration of friction properties; nevertheless, this lubricant reports a lower CoF than lubricants 1 and 2, which represent the proteins solutions (lubricant 1 – simple albumin and lubricant 2 - albumin + γ-globulin solution). The worst CoF is reported by lubricant 1 – simple albumin solution. The rehydration has an expected impact on CoF trend, the CoF value is restarted after each rehydration.

3.2. Visualization of contact

The albumin protein was labelled with all modifications of the lubricant (see Table 1); therefore, all records of the contact area show only albumin dependencies. Snaps were processed by the evaluation software [39] and correspond to one value of CoF; consequently, each snap shows the count of albumin protein clusters and their average size. The evaluation software was calibrated by comparing the trend (tangent slope) of emission intensity (raw output from the experiment – measured by a fluorescent microscope) and the trend (tangent slope) of particle count [39]. The sensitivity of the calibration process to the setting of input parameters is analysed in chapter 4.3. The examples of processed snaps (the protein clusters are highlighted) are shown in Fig. 6; they were taken with lubricant 3 (albumin + γ-globulin + HA – measuring number 5/9). Fig. 6A shows the beginning of the experiment (particles – protein clusters, nearly 1600 clusters of albumin proteins), Fig. 6B represents the state in time t = 25 s (the particle count has increased, nearly 1700 clusters of albumin proteins) and the last

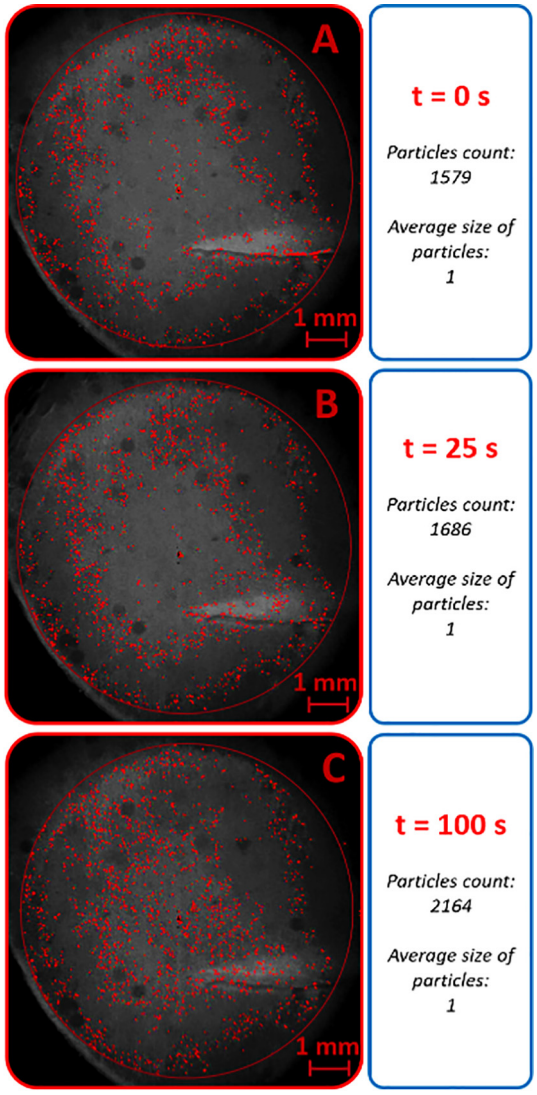

Fig. 6. Snaps of contact area of cartilage – highlighted protein clusters. Experiment with lubricant 3 (albumin + γ-globulin + HA). (A) the start of the experiment – time 0 s, (B) time 25 s, (C) the end of experiment –time 100 s.

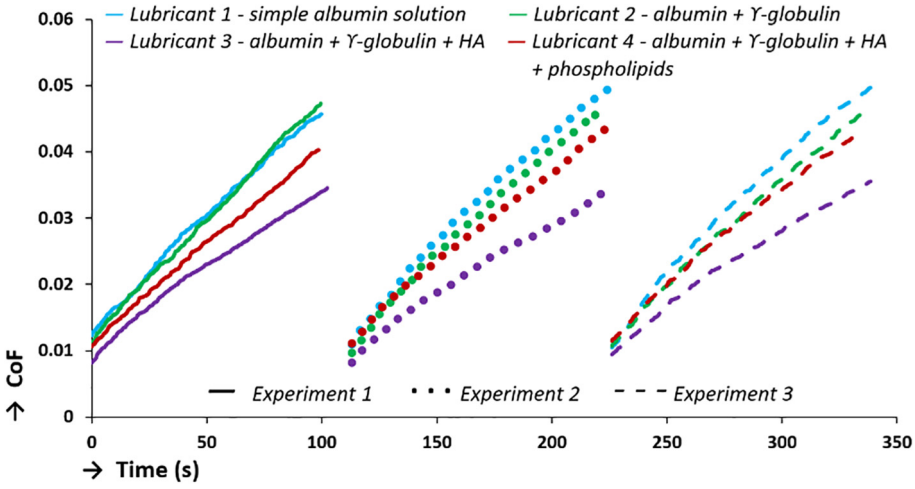

Fig. 5. CoF trends - comparison of all experiments.

snap (Fig. 6C) represents the state at the end of the experiment (the count of protein cluster is the largest, nearly 2200 clusters of albumin proteins). Each of these values belong to one snap. The average size of the detected particles does not change during this experiment. The increase in the particle count is clear from Fig. 6 (the difference between Fig. 6A and Fig. 6B).

The output of evaluation software was determined for each snap in each experimental task so that the particle count trend for each experimental task can be depicted – see Fig. 7. As with CoF trends, one curve in this graph represents 3 averaged measurements, and each type of curve represents one set of experiment (1,2,3) with an in - between rehydration (see Fig. 3). The trends representing protein solutions (lubricant 1 and lubricant 2) show a lower total count of albumin protein clusters than the more complex modification of lubricant 3 and complex SF model – lubricant 4. The trends of lubricant 1 and lubricant 2 mostly show a declining character; however, trends representing more complex modifications of lubricants (lubricant 3 and lubricant 4) show a rising trend of particle count of albumin clusters. Lubricant 3 and lubricant 4 (representing a more complex SF model) show a higher total count of albumin protein clusters than simpler modifications of lubricants (lubricant 1 and lubricant 2). The largest count of albumin protein clusters is shown by lubricant 3 (partial SF – albumin + γ -globulin + HA), although the complex SF model (lubricant 4) reports lower values of protein cluster count.

The particle count does not always have to be an authoritative benchmark for evaluation, quality and quantification of the adsorbed boundary layer; nevertheless, the area of adsorbed boundary layer formed by the labelled component of the lubricant (in this case by albumin protein) has a higher strength of value. The area of the adsorbed boundary layer in the contact is calculated by the multiplication of the particle count and the average size of particles in the contact and is then specified in pixel units. Trends of the albumin adsorbed boundary layer area are shown in Fig. 8. As with CoF trends, one curve in this graph represents 3 averaged measurements, and each type of curve represents one set of experiments (1,2,3) with an in - between rehydration (see Fig. 3). Lubricant 3 (partial SF - albumin + γ-globulin + HA) shows the largest area of the adsorbed boundary layer, although it is not a complex SF model which reports the adsorbed boundary layer mostly with the smallest area. The albumin solution (lubricant 1) shows only a slight reduction in the area of the adsorbed boundary layer. Lubricant 2 (albumin + γ-globulin solution) shows slightly higher values in the area of the adsorbed boundary layer. The adsorbed boundary layer area is further used as an evaluation value for linking the friction in the cartilage contact and its lubrication.

3.3. Connection between friction and lubrication

This study joints two approaches to the evaluation of tribological properties of cartilage - friction evaluation and visualization of cartilage contact. The final output is shown in Fig. 9, where a dependency of friction on lubrication can be seen. The graph shows the impact of friction and also the impact of adsorbed boundary layer; nevertheless, the quality and quantity of adsorbed boundary layer is shown. The larger points in the graph represent the arithmetic mean from one set of measurements (3 individual measurements) and the smaller points represent all experiments carried out. The friction property is represented by *the arithmetic mean of CoF* (x–axis), and the lubrication impact is represented by *the albumin adsorbed boundary layer area* (y-axis). Lubrication is represented by the area of albumin adsorbed boundary layer (count of albumin protein clusters × average size of clusters), which is a representative value expressing formed adsorbed boundary layer. Four shapes can be seen in Fig. 9; each of them represents one lubricant. When the shape is moved closer to the left (closer to the y–axis), the lubricant reports better friction properties and when the shape is moved up (further from the x–axis), the labelled part of the lubricant reports better lubricating properties. The goal is to move the shape as close as possible to the y–axis and as far as possible from the x-axis - as shown by the dashed arrow. Therefore, the best lubricant is number 3 – it is moved further in the direction of the dashed arrow. This lubricant shows the best friction properties while the larger albumin adsorbed boundary layer is formed. Lubricant 4 (complex SF model) shows good tribological properties; however, the adsorbed boundary layer formed by albumin is smaller. Partial SFs (lubricant 1 and lubricant 2) show both inferior frictional and lubricating properties, although the lubricant 1 turns to be slightly better in the area of adsorbed boundary layer. The graph also suggests that the lubricant 3 forms the most stable adsorbed boundary layer because the area of its shape is the smallest; therefore, the measured points are closest to each other. On the contrary, the least stable adsorbed boundary layer is formed by simple albumin solution.

4. Discussion

4.1. Global discussion

A healthy natural synovial joint ensures painless human movement with the phenomenal low friction. The proper function of natural joints is based on the unique properties of cartilage tissue in connection with natural SF [12]. Unfortunately, many diseases

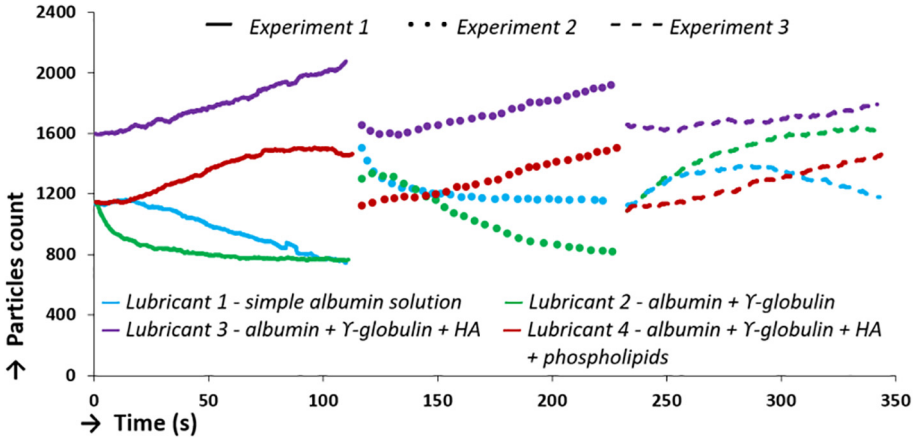

Fig. 7. Particles count trend - comparison of all experiments.

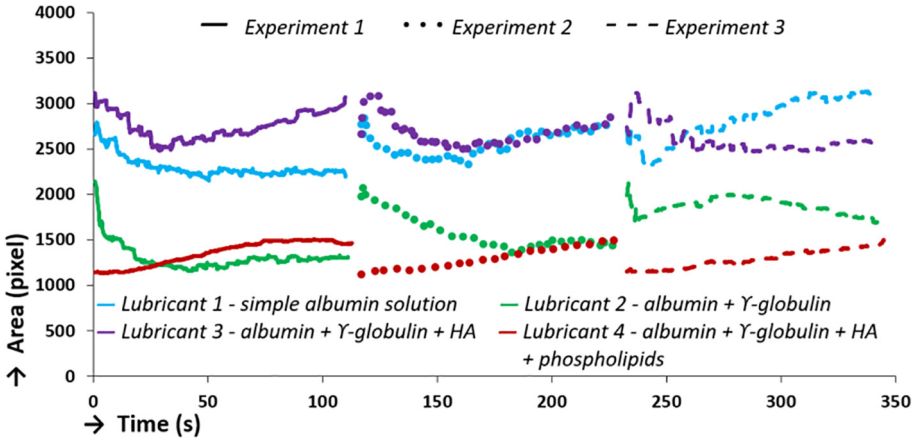

Fig. 8. Trend of adsorbed boundary layer area of albumin - comparison of all experiments.

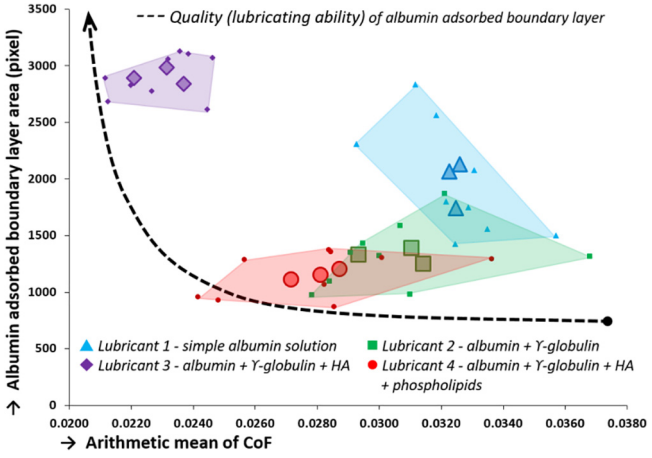

Fig. 9. Dependence of friction on lubrication - arithmetic mean of CoF represent impact of friction and albumin adsorbed boundary layer area represents impact of adsorbed boundary layer.

Table 3
Albumin impact on the lubrication process.

CoF		
Lubricant label deviation	Arithmetic mean	Standard deviation
Lubricant 1	0.0324	0.0016
Lubricant 2	0.0306	0.0025
Lubricant 3	0.0230	0.0012
Lubricant 4	0.0280	0.0027
Particles count in the contact		
Lubricant label	Arithmetic mean	Standard deviation
Lubricant 1	656	485
Lubricant 2	772	291
Lubricant 3	1908	138
Lubricant 4	1155	188
Lubrication film area		
Lubricant label	Arithmetic mean	Standard deviation
Lubricant 1	1980	471
Lubricant 2	1321	276
Lubricant 3	2907	183
Lubricant 4	1158	190

cause degradation and painfulness of joints [1]. The diseases affecting the joints can degrade up to the state when the human movement is not possible without pain. In this case, it is necessary to replace the degraded joint by the artificial one using surgery [2]. The artificial joints do not have an unlimited lifetime; the reoperation is possible but not indefinitely [3]. This is the reason why it is beneficial to postpone the necessity of surgery and stabilize the disease as early as possible. The explanation of cartilage lubricating system is exceedingly substantial for description of lubricating system in natural synovial joint; this knowledge helps to find effective drugs to cure in the best case or, at least, to stabilize or slowdown the disease of natural joints. This study deals with the adsorbed boundary layer formation in the simplified model of synovial joint and describe the role of albumin protein in the SF model.

The global impact of albumin on the lubricating process can be seen in Fig. 9; it is obvious from the shape size that the adsorbed boundary layer formed by the albumin protein is not stable when a simple protein solution is used as lubricant (lubricants 1 and 2). These lubricants show a high standard deviation (see Fig. 9 and Table 3); however, it drops when the lubricants are more complex (lubricants 3 and 4), which is also evident from the area size of individual shapes in Fig. 9. The complex SF model (lubricant 4) and lubricant 3 show lower values of average CoF than simple protein solutions representing lubricants 1 and 2. When the simple albumin solution was used (lubricant 1), the number of protein clusters is declining during the experiment (see in Fig. 7); nevertheless, the average size of its clusters is rising (see in Fig. 8), which causes a slightly increasing area of albumin adsorbed boundary layer in the contact. Simple albumin creates an adsorbed film on hydrophilic surfaces [47]. The cartilage tissue is of a porous structure, whose polarity attracts and absorbs water solutions [48]; therefore, the cartilage surface is suitable for albumin protein adsorption. One part of the lubricant flows through the contact, where the proteins adsorb on the cartilage surface and the other parts flow through the cartilage pores [49]. The albumin proteins create larger clusters when the pressure gradient is higher (in the centre of the contact). It is the reason why the protein clusters on the cartilage contact are smaller than in the case of artificial joints [42]. The increase in the size of albumin protein clusters, and thus also in the area of albumin film, causes, in our opinion, the CoF trend to grow faster and due to the average value of CoF, it is the highest (Fig. 5 and Table 3). The schema of adsorbed boundary layer formation in the case of lubrication by a simple albumin solution (lubricant 1) is shown in Fig. 10-A.

The second variant of the lubricant (lubricant 2) with an added γ–globulin component (see Table 1) shows lower values of CoF than lubricant 1 with albumin only. The particle count also always declines during the experiment (Fig. 7), but the decline is slightly steeper. However, this lubricant shows smaller protein clusters, which causes a lower area of albumin protein film in the contact (Fig. 8). The γ-globulin proteins are much larger than albumin proteins and bind with albumin, as Nečas published in [42]. The albu-

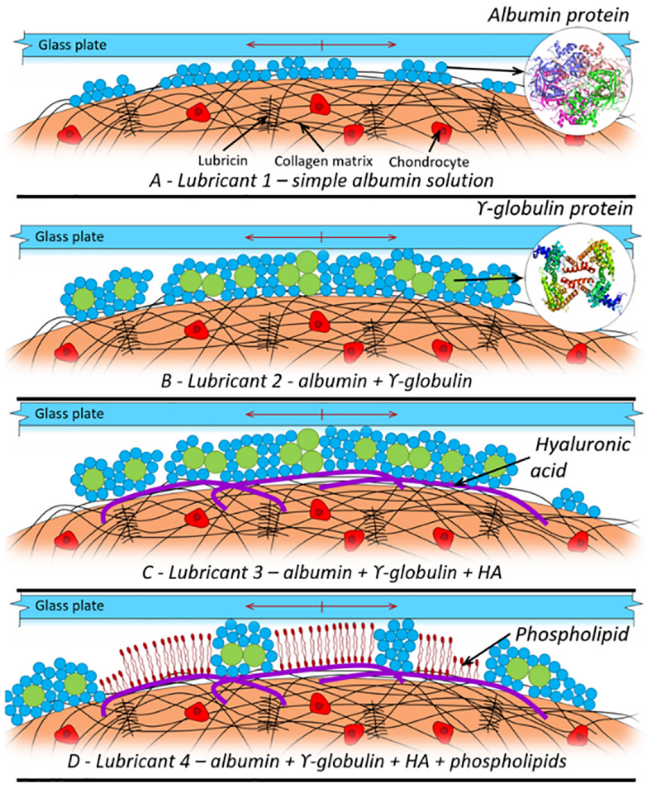

Fig. 10. Schema of adsorbed boundary layer formation. (A) lubricant 1, (B) lubricant 2, (C) lubricant 3, (D) lubricant 4.

min and γ-globulin are proteins characterized by a "string-like" structure. The albumin protein is predominantly characterised by α-helix structure and γ-globulin predominantly by β-sheet [50,51]. These proteins bond together due to their structure - "the string structure becomes entangled in itself" [42,50,51]; therefore, the albumin proteins can bind to the γ-globulin proteins and also the γ-globulin proteins can bond to each other. The adsorbed boundary layer is formed by the albumin cluster, which is divided by γ–globulins; therefore, the cluster formed by albumin is smaller (see Fig. 10-B), where the schema of adsorbed boundary layer formed by lubricant 2 is shown. In our opinion, the combination of albumin clusters and larger γ–globulins causes a greater thickness of the adsorbed boundary layer, leading to lower values of CoF. This deduction is supported also by [35], where the simple γ-globulin shows lower values of CoF.

The lowest values of CoF are produced by lubricant 3, where HA was added. The HA plays an extremely important role in the lubricating system of cartilage [35,49,10] and forms the gel-like layer on the cartilage surface [29]. The surface layers formed by HA protect the cartilage surface against damage [32] and, due to strong hydrophilicity, create an attracting environment for albumin proteins, which adsorb on the surface with better and stronger hydrophilicity. The lubricant 3 (albumin + γ-globulin + HA) shows the best values of CoF (Fig. 5), but also the best values of the number of albumin clusters in the contact (Fig. 7) and the best area of the adsorbed boundary layer formed by albumin (Fig. 8). The number of albumin protein clusters increases during each experiment with lubricant 3; this indicates that the albumin clusters are trapped on the contact mode during experiments. The area of the albumin film formed in the contact decreases in all experiments, though it seems to increase slightly in the other section. The albumin protein clusters are better bonded to the hyaluronic surface layer, which causes a more appropriate fastening of albumin in the contact. The interaction with protein is most present in high molecular weight HA, which also forms the gel-like layer on the cartilage surface. The HA fraction with lower molecular weight penetrated the cartilage structure, in particular the collagen fibres contained in the cartilage structure [31,32,52]. The connection of constitution units of HA causes a firm grip of HA gel–like layer on the cartilage surface. The highest number of albumin clusters in the contact causes a higher thickness of adsorbed boundary layer; therefore, the hyaluronic protecting surface layer is not present in the contact with the raw cartilage surface on the glass plate. In our opinion, it is the reason of the rapid decline of CoF values. The schema of the adsorbed boundary layer provided by lubricant 3 is shown in Fig. 10-C. As is obvious from Fig. 8, the area of lubricant 3 shape is the smallest, i.e., the HA acts as a stabilizer of the adsorbed boundary layer to achieve the same quality of adsorbed boundary layer in each experiment.

The experiments with complex SF (lubricant 4) showed slightly higher values of CoF and lower values of adsorbed boundary layer area formed by albumin, protein, and particle count. In general, it seems that the complex SF has worse tribological properties than the partial complex SF (lubricant 3); nevertheless, the complex SF model is the only one which shows an increasing trend in the number of albumin protein clusters in the contact and an increasing trend of the area of albumin adsorbed boundary layer. This indicates the increasing amount of adsorbed boundary layer during the experiment, which provides a complete protection against cartilage wear. The phospholipids added to the lubricant bind to the HA surface layer on the cartilage. The phospholipids also interbond by lipid tails [27], which allows for the hydration lubrication. However, this is based on the lipid bilayer on each side of the contact, which assumes the same or, at least, similar hydrophilic surface on the other side of the contact. The experimental model used in our study allows for the visualization of the contact of the glass transparent plate; nevertheless, the glass does not meet the requirement for hydrophilicity of surface. The phospholipids bind only to the cartilage surface, or to HA surface layer; therefore, the hydration lubrication is not applied in this case. The schema of the adsorbed boundary layer formation by lubricant 4 is shown in Fig. 10-D. In our opinion, the albumin clusters bind to the cartilage surface and they are imprisoned between a bilayer of phospholipids, which cause a gradual attachment of albumin proteins in the contact. The interaction between proteins and phospholipids is minimal because the phospholipids are strongly bound to the high polar hydration gel-like HA layer; therefore, the phospholipids do not attract low polar albumin and Y-globulin proteins. The phospholipids contain a negative charge phosphate residue of phosphatidic acid and nonpolar lipids residue. In polar solutions (SF), phospholipids are oriented in bilayers or have a micellar orientation, while the phosphate residue is oriented outside of the layer [11,27,53]. The presence of phospholipids causes the increase in CoF [35]; nevertheless, it depends on the amount of all components of the lubricant. In complex SF model (lubricant 4), the presence of phospholipids causes a higher CoF value but the number of protein clusters and the area of albumin film increases during the experiment. The phosphate nuclei bind to water [27,53], and this, without the presence of the second bilayer, together with the structure of phospholipids, causes the lubricant to flow through the contact with higher resistance. The increasing amount of albumin in the contact seems to be the reason of higher value of CoF, as confirmed in [35], where the result shows the same conclusion. The lubrication provided by the complex SF model (lubricant 4) is the only one that allows for long-term operation while avoiding the stable adsorbed boundary layer in the contact.

One of the unique properties of cartilage is the ability of rehydration. As is obvious from Fig. 5, the rehydration between the individual steps of experiment causes the CoF trend to return to

the initial value after each rehydration. Trends showing the adsorbed boundary layer quality (Fig. 7 and Fig. 8) are obviously also affected by rehydration; the trend of adsorbed boundary layer area formed by albumin protein returns to the initial value after each rehydration unlike in the case of particles count in the contact. The regularity of behaviour is better when the lubricant composition is more complex (lubricant 3 and 4). In our opinion, the irregular influence of albumin particle counts in the contact area by the rehydration after each experiment is caused by the count of albumin particles that are nearby the contact area when the experiment is started. The reason is probably that the albumin and γ-globulin proteins in the simpler protein solutions (lubricants 1 and 2) are not as hydrophilic as HA, which causes less ability of individual proteins to bind to the cartilage surface. The regular behaviour of the CoF trends (the value of CoF after rehydration restores to the initial value) in connection with not entirely regular behaviour of trends of particles count through experiments (the value of particles count after rehydration does not always restore to the initial value) point out that the regularity of CoF is not caused only by albumin proteins but it is also affected by other components of synovial fluid. Future research will offer a complete study of each component of synovial fluid. This can contribute to determination of complete dependency of individual components of synovial fluid on the lubricating behaviour and CoF.

4.2. Methodology limitation

The main aim of this study is measuring of friction effects while visualizing the cartilage contact area. The main premiss of this measurement is that one of the contact pairs has to be transparent (the glass plate). The glass plate allows for the reciprocating tribometer to create the model of the synovial joint and allows for the in-situ view of the lubricating processes in the contact. This study admits that the simplified model of synovial joints represents only a very simplified natural synovial joint; however, neither friction measurement nor visualization in-situ can be carried out. In this case, only half of the real joint is preserved – the cartilage sample. The limitation is the elasticity modulus of the glass plate, which is many times higher than the modulus of the second real joint pair, and of different structural, tribological, and hydrophilic properties. Another limitation is the operating condition, which respects the actual pressure in the human joints and the average sliding speed between bones; nevertheless, the variable load cycle, as in the natural joint, is not applied. The values of contact pressure were determined on the basis of maximum values prevailing in the human hip joint; however, the cartilage samples were removed from pigs' joint. To sum up, considering all limitations, the results can only zoom the real adsorbed boundary layer formed in the synovial joint.

As with all experimental bio-tribological tasks, there is a problem with repeatability of measurements performed with the same lubricant but another cartilage sample because each cartilage has a different modulus of elasticity, geometry, and other properties [38]. It is the reason why the measurements were performed on cartilage samples. The aim of this study is to compare the performed measurements and evaluate the data obtained in experiments. The use of a unique sample of cartilage for each measurement could cause the difference between the data from each experiment, especially in visualization, which makes the comparison very difficult. The risk of using one sample is that it can affect consecutive measurements due to the clinging of individual components of the lubricant in the porous structure of cartilage. The components can have a chemical bond to its structure which is very difficult to remove. This study tries to prevent this influence by the initial run-in cycle before each experiment in order to remove all undesired residues from the cartilage structure.

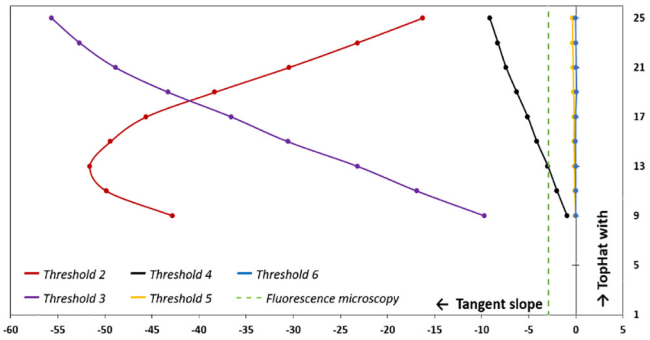

Fig. 11. Sensitivity of processing software settings.

Another provision how to protect the experiment from being influenced by the previous experiment is to determine the lubricant with gradual addition of individual components. Thus the acceptable repeatability can be achieved, see Table 3. The standard deviations of frictional measurements – expected by the CoF, report a magnitude smaller value than the CoF average value – in units of percent. The corresponding value from the assessment of friction/lubrication properties of the lubricant is the CoF; in both cases, it is the area of albumin adsorbed boundary layer calculated from the particle count of albumin protein clusters in the contact and the average size. The arithmetic average and its standard deviation are shown in Table 3.

A part of the experimental apparatus is a specially designed software for processing the snaps from the visualization by fluorescence microscope; a detailed description was published in [39]. For the processed snaps, the software results (particle count and average size of protein clusters) depend on the setting of the input parameters, especially "*TopHat width*" and "*Threshold*". The important input parameters affect the processed snaps; nevertheless, a degree of influence depends on the settings of software. It is calibrated before each experimental set based on the fluorescence trend; however, the calibration may vary depending on the quality of records from the camera, etc. To clarify the magnitude of the effect of variation of input parameters on the software, the sensitivity analysis was performed. The graph in Fig. 11 shows the dependency of the software input parameters in correlation with fluorescence microscopy (dashed green line in Fig. 11). The setting determined for this study is *Threshold* 13, *TopHat width* 4 and the calibration parameter is the tangent slope of intensity trend gained from the fluorescence record; therefore, the settings for these experiments are almost ideal. The set input parameters respond very well; nevertheless, it is not possible to set absolutely the same input parameters as has the intensity trend. Although the input parameters are set to "error", the dependency of other sets is linear; at least in the area (*Threshold* 4). If different input parameters were set (the processing error is linear), the processing error would be deducted because the whole set is processed by one set of input parameters of software.

5. Conclusions

The presented results used the new evaluation procedure introduced in the previous study [39]. This evaluation method allows for simultaneous friction measurement and visualization of contact. The connection of these two previously unconnected tribological approaches contributes to a deeper understanding of tribological behaviour of natural synovial joint including the impact of lubrication on the friction. This research presents a complex study of the impact of albumin protein on the lubrication process of natural cartilage. Fluorescence microscopy, a specially

designed tribometer and evaluation software allow to determine the amount of albumin clusters in the active contact and their average size. The output of visualization is connected to simultaneously measured friction forces, which allows to determine the impact of individual components of the lubricant (albumin in the SF) on the CoF and adsorbed boundary layer formation. Four sets of experiments were carried out, each with one lubricant. The SF model was gradually built from a simple albumin solution to a complex SF model. The concentration corresponds to physiological SF.

The basis of the results are trends of CoF and their relationship with trends represent a lubrication behaviour – the particles count of albumin in the contact and the area of adsorbed boundary layer formed by the albumin protein. The best tribological behaviour was found with lubricant 4, which represents a complex model of synovial fluid. This is the only lubricant which shows low values of friction and a stable adsorbed boundary layer – a permanently rising area of adsorbed boundary layer created by albumin protein. The lubricating behaviour of complex synovial fluid is apparently caused by the presence of HA in combination with phospholipids. In our opinion, HA, due to high hydrophilicity, binds to phospholipids, which causes detention of proteins in the contact. Although the fully complex lubricant represents a good long - term protection of cartilage surface, better friction properties were shown by the lubricant without phospholipids (albumin + γ-globulin + HA). However, a long - term protection of raw cartilage surface is not guaranteed. Although the trends of particles count of albumin in the contact rise quite steeply, the area of albumin adsorbed boundary layer is not always rising over time; the adsorbed boundary layer is likely to break and the raw cartilage surface comes into contact with the glass – the cartilage tissue can be damaged. In the case of protein solutions (simple albumin on one hand and a combination of albumin + γ-globulin on the other hand), a stable adsorbed boundary layer was not observed. In the both cases, the trends of albumin particle counts were decreasing; however, relatively high values of albumin adsorbed boundary layer area were observed, especially for simple albumin lubrication. The trends representing the lubricating quantity in these two cases are not guaranteed. This behaviour seems to be caused by absence of HA, which allows for stronger bonding of proteins with the cartilage surface in the contact. The particles count of albumin and also the area of albumin adsorbed boundary layer show low values for the lubricant combining albumin and γ-globulin. The adsorbed boundary layer consists of a smaller number of particles with a smaller size. The γ–globulin protein is compared to the albumin protein much larger and, based on the previous studies, the γ-globulin binds with albumin. This indicates γ–globulin as a separator of albumin adsorbed boundary layer. The impact of rehydration was also evaluated. The CoF trends return to the initial values after each experiment but the trends representing the adsorbed boundary layer do not show the same trend. This indicates that the restart of CoF values is not only affected by the albumin protein lubrication, but another component is also involved.

The authors presented the first study where the visualization of albumin protein in cartilage contact was performed simultaneously with friction measurement and a newly developed method [39] was used for evaluation of adsorbed boundary layer in a simplified synovial joint model. These methodologies and experimental devices allow for certain limitations and represent not only a simplified model of synovial joints; regardless of this knowledge, this can contribute to the understanding of the lubrication system prevalent in the human synovial joint. In order to approximate the real situation on the nature synovial joint, the future experiments will focus on the evaluation of all components contained in SF. Furthermore, our research assumes the improvement of the experimental equipment using a hydrogel instead of glass, which bring the experimental device closer to the real synovial joint. Newly acquired knowledge gained through a special evaluation method and experimental equipment also allows for a new opportunity in the field of soft contact research (tribology of the eyes, fascia or tissue).

Declaration of Competing Interest

The authors declare that they have no known competing financial interests or personal relationships that could have appeared to influence the work reported in this paper.

Acknowledgement

This research was funded by Czech Science Foundation, grant number 20-00483S.

References

[1] P.A. Simkin, D.O. Graney, J.J. Fiechtner, Roman arches, human joints, and disease, Arthritis Rheum. 23 (11) (1980) 1308–1311, https://doi.org/10.1002/art.1780231114.
[2] J. Buckwalter, J. Martin, Osteoarthritis☆, Adv. Drug Deliv. Rev. 58 (2) (2006) 150–167, https://doi.org/10.1016/j.addr.2006.01.006.
[3] A. Threlkeld, D. Currier, Osteoarthritis, Phys. Ther. 68 (1988) 364–370, https://doi.org/10.1093/ptj/68.3.364.
[4] A. Suckel, F. Geiger, L. Kinzl, N. Wulker, M. Garbrecht, Long-term Results for the Uncemented Zweymuller/Alloclassic Hip Endoprosthesis, J. Arthroplast. 24 (6) (2009) 846–853, https://doi.org/10.1016/j.arth.2008.03.021.
[5] PICONI C, MACCAURO1 G, MURATORI1 F, BRACH DEL PREVER E. Alumina and Zirconia Ceramics in Joint Replacements. Journal of Applied Biomaterials & Biomechanics 2003:19-32. https://doi.org/10.1177/228080000300100103.
[6] N. Bellamy, J. Campbell, V. Welch, T. Gee, R. Bourne, G. Wells, Viscosupplementation for the treatment of osteoarthritis of the knee, Cochrane Database of Systematic Reviews (2006), https://doi.org/10.1002/14651858.CD005321.pub2.
[7] K.D. Brandt, J.A. Block, J.P. Michalski, L.W. Moreland, J.R. Caldwell, P.T. Lavin, Cite Share Favorites Permissions Efficacy and Safety of Intraarticular Sodium Hyaluronate in Knee Osteoarthritis, Clin. Orthop. Relat. Res. 385 (2001) 130–143.
[8] J.A. Jarcho, D.J. Hunter, Viscosupplementation for Osteoarthritis of the Knee, N. Engl. J. Med. 372 (11) (2015) 1040–1047, https://doi.org/10.1056/NEJMct1215534.
[9] R.R. Bannuru, E.E. Vaysbrot, M.C. Sullivan, T.E. McAlindon, Relative efficacy of hyaluronic acid in comparison with NSAIDs for knee osteoarthritis: A systematic review and meta-analysis, Semin. Arthritis Rheum. 43 (5) (2014) 593–599, https://doi.org/10.1016/j.semarthrit.2013.10.002.
[10] D. Rebenda, M. Vrbka, P. Čípek, E. Toropitsyn, D. Nečas, M. Pravda, M. Hartl, On the Dependence of Rheology of Hyaluronic Acid Solutions and Frictional Behavior of Articular Cartilage, Materials 13 (2020) 1–14, https://doi.org/10.3390/ma13112659.
[11] S. Jahn, J. Seror, J. Klein, Lubrication of Articular Cartilage, Annu. Rev. Biomed. Eng. 18 (1) (2016) 235–258, https://doi.org/10.1146/annurev-bioeng-081514-123305.
[12] S.V. Eleswarapu, N.D. Leipzig, K.A. Athanasiou, Gene expression of single articular chondrocytes, Cell Tissue Res. 327 (1) (2006) 43–54, https://doi.org/10.1007/s00441-006-0258-5.
[13] A.J. Almarza, K.A. Athanasiou, Design Characteristics for the Tissue Engineering of Cartilaginous Tissues, Ann. Biomed. Eng. 32 (1) (2004) 2–17, https://doi.org/10.1023/B:ABME.0000007786.37957.65.
[14] M.M. Blum, T.C. Ovaert, Investigation of friction and surface degradation of innovative boundary lubricant functionalized hydrogel material for use as artificial articular cartilage, Wear 301 (1-2) (2013) 201–209, https://doi.org/10.1016/j.wear.2012.11.042.
[15] T.J. Knobloch, S. Madhavan, J. Nam, S. Agarwal, Jr., S. Agarwal, Regulation of Chondrocytic Gene Expression by Biomechanical Signals. Critical Reviews™ in Eukaryotic, Gene Expr. 18 (2) (2008) 139–150, https://doi.org/10.1615/CritRevEukarGeneExpr.v18.i2.30.
[16] J. Becerra, J.A. Andrades, E. Guerado, P. Zamora-Navas, J.M. López-Puertas, A.H. Reddi, Articular Cartilage: Structure and Regeneration, Tissue Eng. Part B Rev. 16 (6) (2010) 617–627, https://doi.org/10.1089/ten.teb.2010.0191.
[17] M.E. Blewis, G.E. Nugent-Derfus, T.A. Schmidt, B.L. Schumacher, R.L. Sah, A MODEL OF SYNOVIAL FLUID LUBRICANT COMPOSITION IN NORMAL AND INJURED JOINTS, Eur. Cells Mater. 13 (2007) 26–39.
[18] T. Schmid, J. Su, K. Lindley, V. Soloveychik, L. Madsen, J. Block, K. Kuettner, B. Schumacher, Superficial zone protein (SZP) is an abundant glycoprotein in human synovial fluid with lubricating properties, in: V. Hascall, K. Kuettner (Eds.), The Many Faces of Osteoarthritis, 1 ed.,., Birkhäuser Basel, Basel, 2002, pp. 159–161, https://doi.org/10.1007/978-3-0348-8133-3_16.

[19] I.M. Schwarz, B.A. Hills, Surface-active phospholipid as the lubricating component of lubricin, Rheumatology 37 (1) (1998) 21–26, https://doi.org/10.1093/rheumatology/37.1.21.
[20] A. Galandáková, J. Ulrichová, K. Langová, A. Hanáková, M. Vrbka, M. Hartl, J. Gallo, Characteristics of synovial fluid required for optimization of lubrication fluid for biotribological experiments, J. Biomed. Mater. Res. B Appl. Biomater. 105 (6) (2017) 1422–1431, https://doi.org/10.1002/jbm.b.33663.
[21] K.A. Athanasiou, M.P. Rosenwasser, J.A. Buckwalter, T.I. Malinin, V.C. Mow, Interspecies comparisons of in situ intrinsic mechanical properties of distal femoral cartilage, J. Orthop. Res. 9 (3) (1991) 330–340, https://doi.org/10.1002/jor.1100090304.
[22] M. MacConaill, The Function of Intra-Articular Fibrocartilages, with Special Reference to the Knee and Inferior Radio-Ulnar Joints, Jurnal of Anatomy 1932 (1932) 220–227.
[23] B.A. Hills, Boundary lubrication in vivo, Proc. Inst. Mech. Eng. [H] 214 (1) (2000) 83–94, https://doi.org/10.1243/0954411001535264.
[24] E.L. Radin, D.A. Swann, P.A. Weisser, Separation of a Hyaluronate-free Lubricating Fraction from Synovial Fluid, Nature 228 (5269) (1970) 377–378, https://doi.org/10.1038/228377a0.
[25] C.W. McCUTCHEN, Mechanism of Animal Joints: Sponge-hydrostatic and Weeping Bearings, Nature 184 (4695) (1959) 1284–1285, https://doi.org/10.1038/1841284a0.
[26] K. Ikeuchi, Origin and future of hydration lubrication, Proceed. Instit. Mech. Eng. Part J: J. Eng. Tribol. 221 (3) (2007) 301–305, https://doi.org/10.1243/13506501JET214.
[27] J. Klein, Hydration lubrication, Hydration lubrication. Friction 1 (1) (2013) 1–23, https://doi.org/10.1007/s40544-013-0001-7.
[28] T. Murakami, Importance of adaptive multimode lubrication mechanism in natural and artificial joints, Proceed. Instit. Mech. Eng. Part J J. Eng. Tribol. 226 (10) (2012) 827–837, https://doi.org/10.1177/1350650112451377.
[29] T. Murakami, S. Yarimitsu, N. Sakai, K. Nakashima, T. Yamaguchi, Y. Sawae, Importance of adaptive multimode lubrication mechanism in natural synovial joints, Tribol. Int. 113 (2017) 306–315, https://doi.org/10.1016/j.triboint.2016.12.052.
[30] S. Yarimitsu, K. Nakashima, Y. Sawae, T. Murakami, Influences of lubricant composition on forming boundary film composed of synovia constituents, Tribol. Int. 42 (11-12) (2009) 1615–1623, https://doi.org/10.1016/j.triboint.2008.11.005.
[31] R. Forsey, J. Fisher, J. Thompson, M. Stone, C. Bell, E. Ingham, The effect of hyaluronic acid and phospholipid based lubricants on friction within a human cartilage damage model, Biomaterials 27 (26) (2006) 4581–4590, https://doi.org/10.1016/j.biomaterials.2006.04.018.
[32] T.-T. Wu, X.-q. Gan, Z.-B. Cai, M.-H. Zhu, M.-T. Qiao, H.-Y. Yu, The lubrication effect of hyaluronic acid and chondroitin sulfate on the natural temporomandibular cartilage under torsional fretting wear, Lubr. Sci. 27 (1) (2015) 29–44, https://doi.org/10.1002/ls.1253.
[33] Y. Merkher, S. Sivan, I. Etsion, A. Maroudas, G. Halperin, A. Yosef, A rational human joint friction test using a human cartilage-on-cartilage arrangement, Tribol. Lett. 22 (1) (2006) 29–36, https://doi.org/10.1007/s11249-006-9069-9.
[34] F. Li, A. Wang, C. Wang, Analysis of friction between articular cartilage and polyvinyl alcohol hydrogel artificial cartilage, J. Mater. Sci. - Mater. Med. 27 (2016) 1–8, https://doi.org/10.1007/s10856-016-5700-y.
[35] D. Furmann, D. Nečas, D. Rebenda, P. Čípek, M. Vrbka, I. Křupka, M. Hartl, The Effect of Synovial Fluid Composition, Speed and Load on Frictional Behaviour of Articular Cartilage, Materials 13 (2020) 1–16, https://doi.org/10.3390/ma13061334.
[36] A. Moore, D. Burris, New Insights Into Joint Lubrication, Tribol. Lubricat. Technol. 72 (2016) 26–30.
[37] A.C. Cilingir, Effect of rotational and sliding motions on friction and degeneration of articular cartilage under dry and wet friction, J. Bionic Eng. 12 (3) (2015) 464–472, https://doi.org/10.1016/S1672-6529(14)60137-2.
[38] S.M.T. Chan, C.P. Neu, G. DuRaine, K. Komvopoulos, A.H. Reddi, Atomic force microscope investigation of the boundary-lubricant layer in articular cartilage, Osteoarth. Cartil. 18 (7) (2010) 956–963, https://doi.org/10.1016/j.joca.2010.03.012.
[39] P. Čípek, M. Vrbka, D. Rebenda, D. Nečas, I. Křupka, Biotribology of Synovial Cartilage: A New Method for Visualization of Adsorbed boundary layer and Simultaneous Measurement of the Friction Coefficient, Materials 13 (2020) 1–19, https://doi.org/10.3390/ma13092075.
[40] Development of reciprocating tribometer for testing synovial joint. ENGINEERING MECHANICS 2018, Svratka, Czech republic: Engineering Mechanics; 2018, pp. 169-172. https://doi.org/10.21495/91-8-169.
[41] P. Čípek, D. Rebenda, D. Nečas, M. Vrbka, I. Křupka, M. Hartl, Visualization of Adsorbed boundary layer in Model of Synovial Joint, Tribol. Industry 41 (2019) 387–393.
[42] D. Nečas, M. Vrbka, A. Galandáková, I. Křupka, M. Hartl, On the observation of lubrication mechanisms within hip joint replacements. Part I: Hard-on-soft bearing pairs, J. Mech. Behav. Biomed. Mater. 89 (2019) 237–248, https://doi.org/10.1016/j.jmbbm.2018.09.022.
[43] D. Nečas, M. Vrbka, F. Urban, I. Křupka, M. Hartl, The effect of lubricant constituents on lubrication mechanisms in hip joint replacements, J. Mech. Behav. Biomed. Mater. 55 (2016) 295–307, https://doi.org/10.1016/j.jmbbm.2015.11.006.
[44] J.E. Pickard, J. Fisher, E. Ingham, J. Egan, Investigation into the effects of proteins and lipids on the frictional properties of articular cartilage, Biomaterials 19 (19) (1998) 1807–1812, https://doi.org/10.1016/S0142-9612(98)00147-1.
[45] W. Hodge, R. Fijan, K. Carlson, R. Burgess, W. Harris, R. Mann, Contact pressures in the human hip joint measured in vivo, Proc. Natl. Acad. Sci. 83 (2879–2883) (1986) 2879–2883, https://doi.org/10.1073/pnas.83.9.2879.
[46] V.C. Mow, A. Ratcliffe, A. Robin Poole, Cartilage and diarthrodial joints as paradigms for hierarchical materials and structures, Biomaterials 13 (2) (1992) 67–97, https://doi.org/10.1016/0142-9612(92)90001-5.
[47] Y.L. Jeyachandran, E. Mielczarski, B. Rai, J.A. Mielczarski, Quantitative and Qualitative Evaluation of Adsorption/Desorption of Bovine Serum Albumin on Hydrophilic and Hydrophobic Surfaces, Langmuir 25 (19) (2009) 11614–11620, https://doi.org/10.1021/la901453a.
[48] S.M. McNary, K.A. Athanasiou, A.H. Reddi, Engineering Lubrication in Articular Cartilage, Tissue Eng. Part B: Rev. 18 (2) (2012) 88–100, https://doi.org/10.1089/ten.teb.2011.0394.
[49] G.W. Greene, B. Zappone, B. Zhao, O. Söderman, D. Topgaard, G. Rata, J.N. Israelachvili, Changes in pore morphology and fluid transport in compressed articular cartilage and the implications for joint lubrication, Biomaterials 29 (33) (2008) 4455–4462, https://doi.org/10.1016/j.biomaterials.2008.07.046.
[50] S.B. Dev, J.T. Keller, C.K. Rha, Secondary structure of 11 S globulin in aqueous solution investigated by FT-IR derivative spectroscopy, Biochim. et Biophys. Acta (BBA) - Protein Struct. Molecul. Enzymol. 957 (2) (1988) 272–280, https://doi.org/10.1016/0167-4838(88)90283-X.
[51] M.J. Howard, C.M. Smales, NMR Analysis of Synthetic Human Serum Albumin α-Helix 28 Identifies Structural Distortion upon Amadori Modification, J. Biol. Chem. 280 (24) (2005) 22582–22589, https://doi.org/10.1074/jbc.M501480200.
[52] Z. Liu, W. Lin, Y. Fan, N. Kampf, Y. Wang, J. Klein, Effects of Hyaluronan Molecular Weight on the Lubrication of Cartilage-Emulating Boundary Layers, Biomacromolecules 21 (10) (2020) 4345–4354, https://doi.org/10.1021/acs.biomac.0c0115110.1021/acs.biomac.0c01151.s001.
[53] R. Murray, D. Granner, P. Mayes, V. Rodwell, Harper's Illustrated Biochemistry, 28 ed., McGraw-Hill, New York, United States, 2018.